analytical chemistry

Subscriber access provided by Stockholm University Library

Article

CRISPR-Cas12a Coupled with Platinum Nano-Reporter for Visual Quantification of SNVs on a Volumetric Bar-Chart Chip

Ning Shao, Xin Han, Yanni Song, Pengchao Zhang, and Lidong Qin

Anal. Chem., **Just Accepted Manuscript** • DOI: 10.1021/acs.analchem.9b02925 • Publication Date (Web): 28 Aug 2019

Downloaded from pubs.acs.org on August 28, 2019

Just Accepted

"Just Accepted" manuscripts have been peer-reviewed and accepted for publication. They are posted online prior to technical editing, formatting for publication and author proofing. The American Chemical Society provides "Just Accepted" as a service to the research community to expedite the dissemination of scientific material as soon as possible after acceptance. "Just Accepted" manuscripts appear in full in PDF format accompanied by an HTML abstract. "Just Accepted" manuscripts have been fully peer reviewed, but should not be considered the official version of record. They are citable by the Digital Object Identifier (DOI®). "Just Accepted" is an optional service offered to authors. Therefore, the "Just Accepted" Web site may not include all articles that will be published in the journal. After a manuscript is technically edited and formatted, it will be removed from the "Just Accepted" Web site and published as an ASAP article. Note that technical editing may introduce minor changes to the manuscript text and/or graphics which could affect content, and all legal disclaimers and ethical guidelines that apply to the journal pertain. ACS cannot be held responsible for errors or consequences arising from the use of information contained in these "Just Accepted" manuscripts.

is published by the American Chemical Society. 1155 Sixteenth Street N.W., Washington, DC 20036

Published by American Chemical Society. Copyright © American Chemical Society. However, no copyright claim is made to original U.S. Government works, or works produced by employees of any Commonwealth realm Crown government in the course of their duties.

CRISPR-Cas12a Coupled with Platinum Nano-Reporter for Visual Quantification of SNVs on a Volumetric Bar-Chart Chip

Ning Shao,[1, 2, ‡] Xin Han,[1, 2, 3, ‡] Yanni Song,[4] Pengchao Zhang[1, 2] and Lidong Qin[1, 2, *]

[1] Department of Nanomedicine, Houston Methodist Research Institute, 6670 Bertner Ave, Houston, TX 77030, USA. [2] Deartment of Cell and Developmental Biology, Weill Medical College of Cornell University, New York, NY 10065, USA. [3] School of Medicine and Life Sciences, Nanjing University of Chinese Medicine, Nanjing, 210023, China. [4] Department of Breast Surgery, Harbin Medical University Cancer Hospital, Harbin 150081, China.

ABSTRACT: Methods that can detect and quantify single nucleotide variations (SNVs)/single nucleotide polymorphisms (SNPs) are greatly needed in bioanalysis measuring gene mutations and polymorphisms. Herein, a visual and instrument-free SNV quantification platform is developed. Platinum nanoparticles tethered to magnetic beads by single-stranded DNAs are designed as quantitative readout reporters for CRISPR-Cas12a nucleic acid detection system. The integration of platinum nano-reporter and the CRISPR-Cas system with a volumetric bar chart chip realizes volumetric quantification of nucleic acids. This platform enables quantification of multiple cancer mutations in pure DNA samples and mock cell-free DNA samples in serum, with allelic fractions as low as 0.01%. This platform could have great potential in quantification of SNVs/SNPs as well as other types of nucleic acid targets at the point of care.

Identification and quantification of single nucleotide variations (SNVs)/single nucleotide polymorphisms (SNPs) is greatly needed in many areas ranging from detection of disease-related mutations[1,2] to genotyping of human[3,4], animals[5], plants[6] and microbes[7,8]. In the past few decades, many methods have been developed to identify and/or quantify SNVs/SNPs based on different types of technologies[9-15]. These methods are often limited by the long detection time, complicated procedures or dependence on sophisticated instruments. Particularly, quantification of SNVs/SNPs at the point of care is still very challenging to date. Very recently, the clustered regularly interspaced short palindromic repeats (CRISPR) and CRISPR-associated (Cas) nuclease systems have been deployed in nucleic acid detection[16-20]. These systems show great promise by providing high sensitivity, single-base specificity and point-of-care compatibility. Nevertheless, the readout in these systems mainly rely on fluorescent reporters[16,17,19] or lateral flow strips[18,20], both of which provide insufficient quantification capability at the point of care. Simple and quantitative readout methods with point-of-care capability would enhance the performance of CRISPR-based nucleic acid detection methods and broaden their applications.

Microfluidics and nanotechnology have contributed a lot to improve the performance of numerous analytical methods and could also contribute to the newly emerged CRISPR-based detection methods if properly designed. Our laboratory has previously developed a multiplexed volumetric bar chart chip (V-Chip) platform, which employs ink bar charts to measure oxygen produced from the reaction between catalase/platinum nanoparticle (PtNP) and hydrogen peroxide (H_2O_2), realizing direct visual quantification of protein/nucleic acid molecules without instruments or data processing[21-24]. Herein, we report a magnet-assisted V-Chip (MAV-Chip) combined with PtNP reporter and CRISPR-Cas12a for visual and sensitive quantification of SNVs. In this platform, magnetic Bead-single-stranded DNA (ssDNA)-PtNP (BDNP) conjugates were introduced into the CRISPR-Cas12a nucleic acid detection system as a reporter to replace the conventional fluorescent reporter. Once the guide RNA binds to the target DNA, the non-specific ssDNA cleavage of Cas12a is activated and the ssDNA linker in BDNPs is degraded to unleash PtNPs from the magnetic beads. Applying the whole reaction to V-Chip and using a magnet to hold the magnetic bead PtNP conjugates with separating unleashed PtNPs from intact and cleaved BDNPs, PtNP-initiated oxygen production and direct visual quantification of the target could be realized on the MAV-Chip. Multiplex and sensitive quantification of cancer-related SNVs was performed to demonstrate the feasibility and practicality of the platform.

Materials & Methods

Materials

Glass slides (75×50×1 mm) were purchased from Corning Inc. (Corning, NY). SPR220-7 was purchased from MicroChem Corp. (Newton, MA). MF-CD26 was obtained from Rohm and Haas Electronic Materials (Marlborough, MA). Polyvinyl chloride sealing tape was obtained from 3M (St. Paul, MN). H_2O_2 (35% wt in H_2O), NH_4F, HF, HNO_3, bovine serum albumin (BSA), human serum and Tridecafluoro-1,1,2,2-tetrahydrooctyl-1-trichlorosilane were obtained from Sigma-Aldrich, Inc. (St. Louis, MO). Amorphous diamond-coated drill bits (0.031-inch cutter diameter) were purchased from Harvey Tool (Rowley, MA). FC-70 (a mixture of perfluoro-tri-n-butylamine and perfluoro-di-n-butylmethylamine) was purchased from Hampton Research (Aliso Viejo, CA). Lba Cas12a was purchased from New England Biolabs Inc. (Ipswich, MA). DynabeadsTM MyOneTM Streptavidin T1, PierceTM Premium-Grade TCEP HCL and nuclease-free water were purchased from Thermo Fisher Scientific (Waltham, MA).

BioPure™ 5 nm platinum nanoparticle was purchased from nanoComposix Inc. (San Diego, CA). Block magnet (BY0X0X0, 2" x 1" x 1", neodymium) was purchased from K&J Magnetics Inc (Pipersville, PA). PBS buffer (0.1 M, pH7.4) was obtained from Corning, Inc. (Manassas, VA). Food color was obtained from AmeriColor (Placentia, CA). All devices were designed as computer graphics using AutoCAD 2016 software and then printed out as transparency photomasks by CAD/Art Services, Inc. (Bandon, OR) with resolution at 10 μm. All DNA oligomers and guide RNA were synthesized by Integrated DNA Technologies, Inc (Coralville, IA) and listed in Supporting Information. The crRNA needs to be designed to target a sequence with TTTV PAM (V = A, C, or G). Detecting an allele needs PAM mutations or mismatches in PAM-adjacent "seed region"[17].

Fabrication of the V-chip

Standard photolithography process was used to fabricate the V-chip device, as described in our previous studies[22]. In brief, a 10-μm layer of SPR220-7 photoresist was molded on glass slide (75×50×1 mm) as designed, followed by etching with glass etchant (1:0.5:0.75 mol/L $HF/NH_4F/HNO_3$) to get the wells and channels. Holes for loading reagents were then drilled with a diamond drill bit. The glass slides were thoroughly cleaned by Piranha solution (H_2SO_4:H_2O_2 = 3:1), treated with oxygen plasma, and surface-coated with tridecafluoro-1,1,2,2-tetrahydrooctyl-1-trichlorosilane for hydrophobic modification. To minimize the nonspecific binding of BDNPs to the surface of reaction wells, the reaction wells was pre-blocked with BSA.

Operation of the MAV-chip

To assemble the device, five microliters of FC-70 were applied to the top slide of the V-chip with the patterns facing up. The top slide was then assembled with the bottom slide and slid against each other repeatedly to completely spread the FC-70 oil onto the surfaces of the two slides. The ultrathin FC-70 layer served as a binder for sealing of the two glass slides as well as a lubricant for preventing air pockets during sliding. The two slides were then aligned to connect the relevant wells and channels to the inlets and outlets. Reagents were loaded into the channels and wells via pipetting. To obtain readout, the assembled device was put on a flat magnet which could cover the whole area of the reaction wells for one minute to thoroughly drag down the magnetic BDNPs to the bottom wells. The top slide was then slid vertically up to bring reaction solution in the top reaction wells to the gas generating wells filled with H_2O_2. The horizontal fluidic paths were also separated and re-formed into independent units arranged in parallel in the vertical direction as a result of the sliding. In each independent unit, PtNPs released into the reaction solution could react with H_2O_2 and generate oxygen to push red ink moving up in the channels. The results were recorded by the back camera of an Honor V10 cellphone and the frontiers of ink advancement were marked for quantitation.

BDNP conjugation

Conjugation of ssDNA linker with PtNPs was performed according to methods reported previously[25,26]. In brief, disulfide-labeled ssDNA (50 μM) was reduced by TCEP, then mixed with PtNPs (2.4 μM) at a 20:1 molar ratio in the presence of 0.01 M Phosphate Buffer (PB) and 0.01% SDS. The solution was vortexed and identical volume of NaCl (4 M) was added every 20 min to reach a concentration of 1 M after 10 times of adding. The mixture was vortexed for 24 hours more to complete the conjugation. After washing, the DNA-PtNP conjugates and the Streptavidin-coated Dynabeads were pre-incubated in 1% BSA overnight at 4 ℃ individually to avoid nonspecific binding of the DNA-PtNP conjugates to the surface of the Dynabeads. Then the DNA-PtNP conjugates and the Dynabeads were mixed together and vortexed at room temperature for two hours to enable the binding of biotin on the DNA to Streptavidin on the Dynabeads. The BDNP conjugates were then washed with the washing buffer plus 1% BSA for three times, followed by resuspension in washing buffer plus 1% BSA. The final conjugates were stored at 4 ℃ for following experiments.

BDNP characterization

DNA-PtNP conjugates were characterized by both spectrophotometry analysis of the DNA content in the conjugates using Nanodrop (Thermo Fisher Scientific, Waltham, MA)[26] and hybridization with fluorescent-labeled oligo probe[27]. BDNP conjugates were firstly characterized by hybridization with fluorescent-labeled oligo probe. The conjugates before and after Cas12a-mediated cleavage were then prepared respectively and characterized by transmission electron microscopy (TEM). TEM images were obtained on a JEOL JEM-1400 transmission electron microscope (JEOL, USA) at 80 kV.

Preparation of the DNA targets

Sequences of the SNV-contained targets, corresponding wild type sequences and their complementary sequences were obtained from database and synthesized commercially. The SNV-contained or wild type dsDNA targets were prepared by annealing of the two complementary ssDNA using a thermal cycler (Bio-Rad C1000 TouchTM).

SNV detection via fluorophore quencher (FQ)-labeled reporter in 384-well microplate

SNV detection via FQ-labeled reporter was performed according to the reference[17] and the instruction of the manufacturer of LbCas12a. Briefly, LbCas12a-crRNA complexes were preassembled by incubating 200 nM LbCpf1 with 200 nM crRNA at room temperature for 10 min. Afterwards, a desired amount of DNA sample and 200 nM ssDNA FQ reporter were added into the reaction mixture to initiate the reaction. A final concentration of 20 nM LbCas12a, 20 nM crRNA, 20 nM target, 20 nM FQ reporter and 1× NEB2.1 Reaction Buffer is applied in a 20 μL reaction. Reactions (20 μL, 384-well microplate format) were incubated in a fluorescence plate reader (BioTek Synergy H4 Hybrid Reader) for 30 min at 37 °C with fluorescence measurements taken every minute (λex: 485 nm; λem: 535 nm).

SNV detection via BDNP reporter in PCR tubes

The reaction mixture for SNV detection via BDNP reporter was prepared as described above, with the following modifications: BDNP reporter was added into the reaction mixture in replace of the ssDNA FQ reporter. The reaction mixtures were incubated at 37 °C for one hour. After the reaction complete, the PCR tubes were put on a magnetic rack for one minute to separate BDNPs from the solution containing unleashed PtNP. The supernatant was carefully collected and mixed with H_2O_2 in new PCR tubes. Generation of oxygen bubbles was recorded by the back camera of an Honor V10 cellphone.

SNV detection on the MAV-chip via BDNP reporter

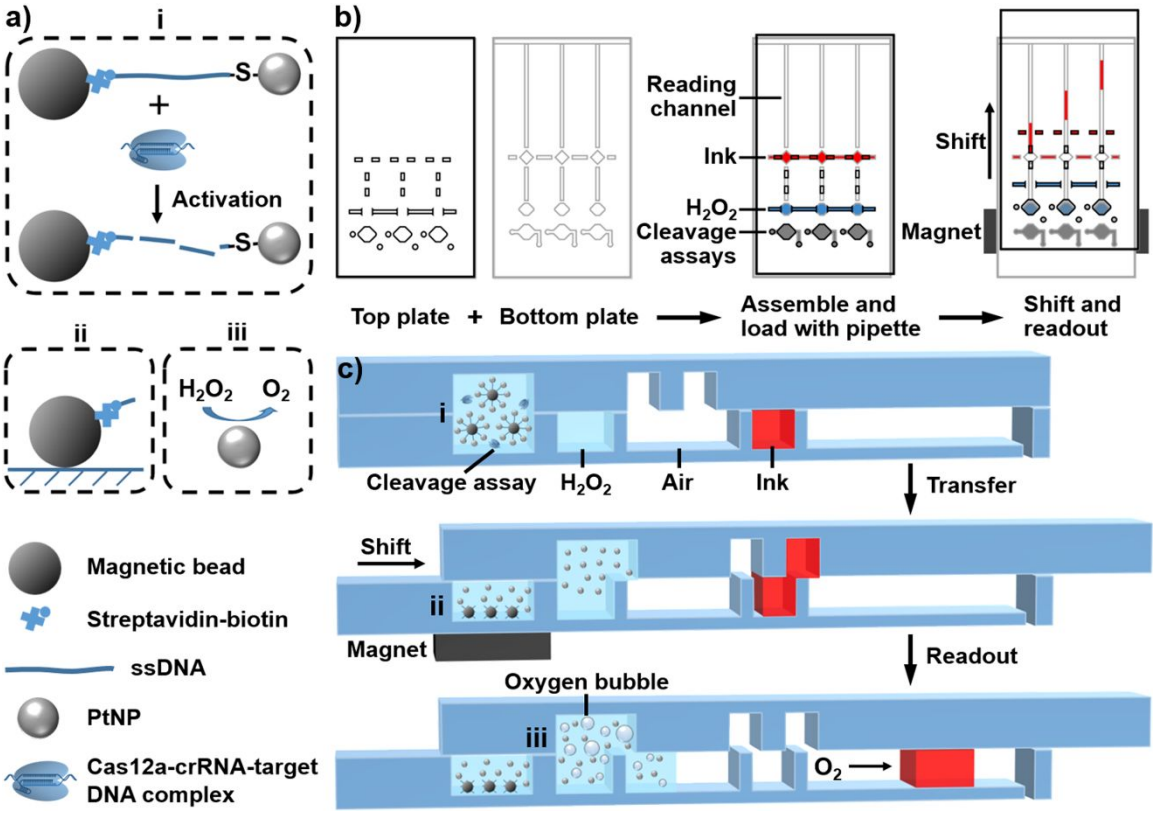


Figure 1. Working principle of the platinum nano-reporter-based CRISPR-Cas12a detection system on the MAV-Chip. (a) Schematic view of the modified CRISPR-Cas12a detection system based on the BDNP reporter. i, ii, iii represent the three key processes in the detection assay, i.e., Cas12a-mediated cleavage of the BDNP reporter, magnetic separation of the intact/partially-reacted BDNP from unleashed PtNPs and oxygen generation catalyzed by PtNPs, respectively. (b) Schematic views of the MAV-Chip design and operation. (c). Schematic cross-section view of the MAV-Chip in the state of assay/reagent loading, shifting and readout.

The reaction mixture was prepared as described above, with the following modifications: Doubled concentrations of LbCas12a and crRNA were applied, as well as a final concentration of 1% BSA was added into the reaction mixture. MAV-chip was pre-blocked and assembled as described above. Two microliters of each reaction mixture were individually loaded into the reaction wells by pipetting through the inlet. The inlets and outlets of the reaction wells were sealed by adding drops of mineral oil on them. The chip was incubated at 37 °C for one hour. Afterwards, 10 μL H_2O_2 and red ink were loaded into their respective fluidic paths by pipetting. The following readout was performed as described above.

The detailed experimental procedures are available in the Supporting Information.

Results

Working principle of the platform. Figure 1a shows the scheme of the modified CRISPR-Cas12a nucleic acid detection system based on the BDNP reporter. The BDNP reporter is synthesized by linking PtNPs to a streptavidin-coated magnetic bead via an ssDNA which is modified with a biotin group on one end and a thiol group on the other end. The biotin binds to the streptavidin with a very strong affinity, while the thiol group reacts with the PtNP via coordination bonding. Once the BDNP reporter is added to CRISPR-Cas12a nucleic acid detection system, specific guide RNA binds to its target DNA and activates indiscriminate single-stranded DNase activity of Cas12a. Activated Cas12a cleaves the ssDNA linker between the PtNP and the magnetic bead (Figure 1a i). After the reaction, the unleashed PtNPs are magnetically separated from the magnetic beads (Figure 1a ii) and transferred to catalyze H_2O_2 to generate oxygen (Figure 1a iii). The amount of produced oxygen indicates the amount of the unleashed PtNPs as well as the amount of the target DNA in the reaction.

To realize the whole idea and achieve visual quantification of the target DNA, we designed the MAV-Chip, shown in Figure 1b and Figure 1c. Firstly, the top plate and the bottom plate are assembled and multiple BDNP reporter-contained Cas12a cleavage assays are loaded into the reaction wells individually. After the reaction, hydrogen peroxide and ink are loaded into their corresponding flow paths respectively. Finally, the top plate is shifted vertically to transfer the reaction solution in the reaction wells of the top plate to the oxygen-generating wells filled with H_2O_2. The horizontal fluidic paths are separated and re-formed into independent vertical fluidic units arranged in parallel during the shifting. A flat magnet is put under the reaction area of the chip during the shifting to make sure that magnetic beads with leashed PtNPs remain in the bottom reaction wells while unleashed PtNPs can be transferred to mix with H_2O_2. The advancements of the red ink bars resulted from the generated oxygen gas indicate the amounts of targets in the corresponding Cas12a cleavage reactions. A schematic cross-section view of the MAV-Chip in the state of assay/ reagent loading, shifting and readout is shown in Figure 1c for clearer demonstration of the reagents handling. Top and bottom plates of a 6-plexed MAV-Chip with dimensions are shown in Figure

S1. Representative pictures of the 6-plex MAV-Chip operation and readout are shown in Figure S2a and Figure S2b, respectively.

Synthesis and characterization of the BDNP conjugates. PtNPs with an average diameter of five nanometers were utilized for the synthesis. A relatively long 100-mer Poly-T ssDNA was synthesized as the linker between the PtNP and the magnetic bead to reduce the steric hindrance during the cleavage of the ssDNA by Cas12a and increase the cleaving efficiency. Poly-T ssDNA with a length of 35 nucleotides was also tested in Cas12a cleavage assays and showed much lower PtNP release (data not shown), probably due to the steric hindrance between streptavidin and PtNP. A scheme of the two-step BDNP conjugation process is shown in Figure S3. Briefly, the ssDNA linker was firstly conjugated to the PtNPs. After washing off unbounded ssDNA and blocking the remaining activate site, the ssDNA-PtNP conjugates were mixed with the streptavidin coated magnetic Dynabeads to form the final BDNP conjugates. Detailed experimental procedures of the BDNP conjugation can be found in the Supporting Information.

To validate the conjugation of ssDNA to PtNPs, the PtNP-ssDNA conjugates and bare PtNPs were hybridized with a fluorescently-labeled 30-mer poly-A probe at 50 ℃ for two hours respectively.[27] After washing, the fluorescent probe was stripped from the conjugates by denaturation at 95 ℃ and immediate ice bath (Figure 2a). Spinning down the conjugates, the stripped fluorescent probe in solution was recovered and then analyzed by fluorescent microscopy. As shown in Figure 2b, the PtNP-ssDNA conjugates resulted in a 22-fold increase of the fluorescence in comparison to the bare PtNPs, indicating successful conjugation of the ssDNA to the PtNPs. The average DNA loading density on a PtNP was further estimated as eight via spectrophotometry analysis of the conjugates and DNA (Figure S4a)[26]. The conjugation of PtNPs to the magnetic bead was confirmed by TEM images. Compared to intact BDNP, cleaved BDNP after the Cas12a-based cleavage assay shows significant decrease in the number of PtNPs on the surface of the magnetic bead, further proved the conjugation is via the ssDNA linker (Figure 2c). The presence of the ssDNA linker in the conjugates was also validated by fluorescent probe hybridization. As expected, BDNPs show much higher fluorescence compared with bare magnetic beads after the hybridization (Figure 2d). The final concentrations of ssDNA and PtNP in BDNPs, as well as the yield of BDNPs were estimated in Figure S4b, c and e. A BDNP yield of ~35% was gained by calculating ratio of the PtNP content in the final BDNPs to the starting PtNP content. This relatively low yield can be mainly explained by the excess amount of the ssDNA-PtNP conjugates that was used to mix with the magnetic beads to maximize the density of PtNP on the magnetic beads. The average PtNP loading density on a magnetic bead was estimated as 1.70-2.43 x 10^4/bead. In our experiments, one milligram of the beads can bind about 280 pmol ssDNA-PtNP conjugates via calculation. As a reference, one milligram of the beads can bind about 500 pmol biotinylated ss-oligonucleotides according to the manufacturer's description. In consideration of the steric hindrance caused by PtNPs, we believe that our conjugation efficiency is comparable to the manufacturer's description.

BDNP can serve as a reporter for Cas12a-based nucleic acid detection system. To further confirm the success of the BDNP conjugation and the feasibility of applying BDNPs to Cas12a-based nucleic acid detection system as a reporter, we

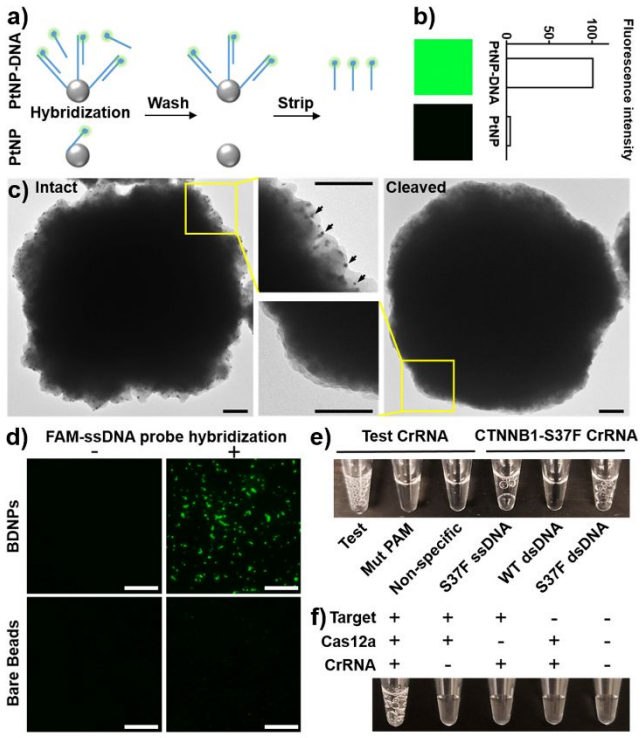


Figure 2. Validation of the BDNP Conjugation and target-activated cleavage of the conjugates by Cas12a. (a) Schematic view of hybridization-based validation of ssDNA-PtNP conjugation. (b) Fluorescent images of the stripped probe solution and quantitation of the fluorescence. (c) Representative TEM images of the intact BDNPs and Cas12a-cleaved BDNPs. PtNPs are marked with arrows in the inset. Scale bars are 100 nm. (d) Representative images of the BDNPs/bare beads before/after hybridized with FAM-labeled ssDNA probe. Scale bars are 25 μm. (e) Oxygen generation for different targets after the modified CRISPR-Cas12a assays based on BDNPs. (f) Oxygen generation for different reaction conditions in which each key component of the reaction was deleted respectively.

synthesized several DNA targets and corresponding guide RNAs. BDNPs were introduced into the Cas12a-based detection assays to test if detection of these DNA targets could be achieved via oxygen production resulted from the PtNPs unleashed from the BDNPs. After the cleavage reaction, a magnetic rack was applied to separate magnetic beads from other components in solution, including the unleashed PtNPs. The supernatants were then recovered and mixed with H_2O_2 in PCR tubes to observe the generation of oxygen bubbles. A pair of sequences (i.e., Test and its protospacer adjacent motif (PAM) mutant (Mut-PAM)) reported in the literature was first employed for the testing[17]. As shown in Figure 2e left, oxygen production was observed in the tubes that contained supernatants from the Test sequence-contained reaction, but not in the tubes that contained supernatants from the PAM mutant sequence-contained reaction or from the non-specific sequence-contained reaction. This result not only further confirmed the success of BDNP conjugation but also demonstrate the functionality and sequence specificity of the modified Cas12a detection system. By testing another group of DNA targets including wild type double-stranded DNA (dsDNA) of CTNNB1 (catenin beta 1) and its corresponding dsDNA contains the S37F mutation, we demonstrated that the guide RNA which is specific to the S37F mutation clearly

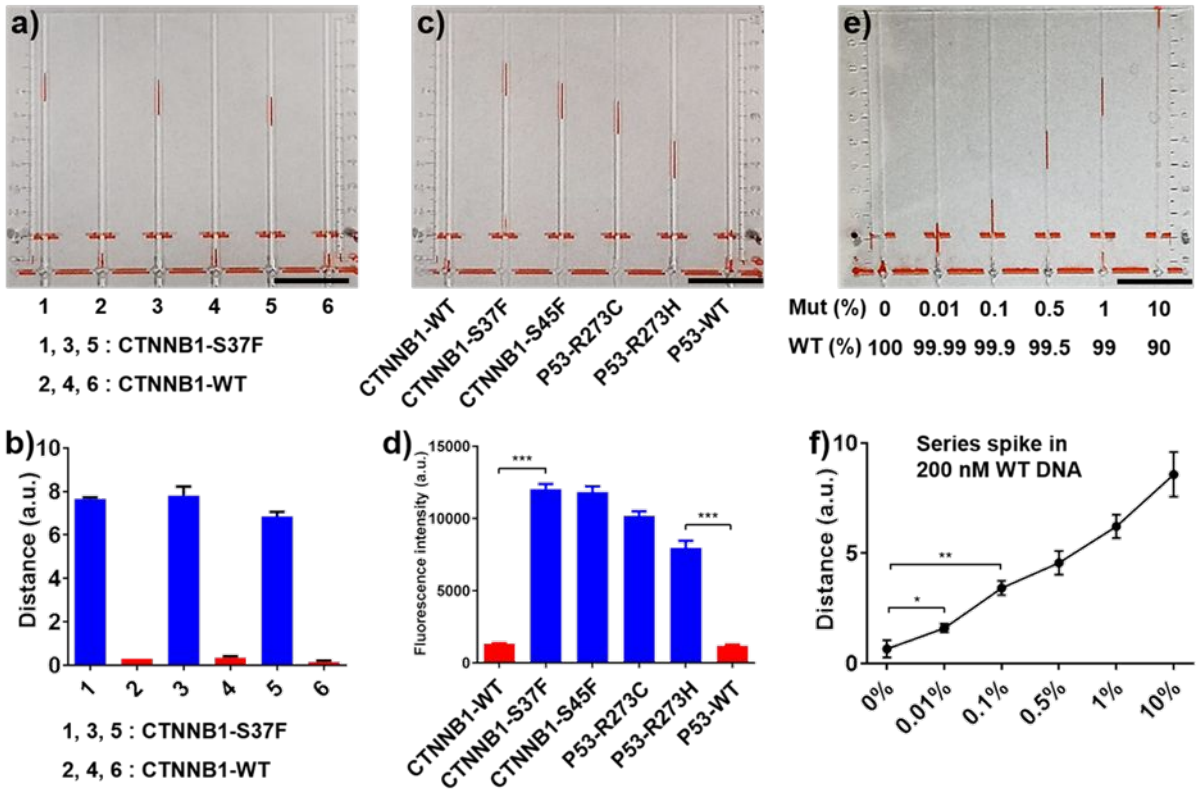


Figure 3. Visual detection of single nucleotide variations on the MAV-Chips. (a, b) Uniformity of the MAV-Chip-based detection platform demonstrated by detection of CTNNB1-S37F mutant dsDNA and its wild type dsDNA. (c) Multiplex detection of four SNVs on a MAV-Chip. Corresponding wild type DNAs were also applied as controls. (d) Detection of the four SNVs using fluorescent reporter enabled the Cas12a-based detection method. (e, f) Detection limit of the MAV-Chip platform for detecting SNVs in background DNAs. Scale bars are 1 cm for (a), (c) and (e). (b), (d) and (f), n = three technical replicates, two-tailed Student's t test; *P<0.05, **P<0.01, and ***P < 0.001; error bars represent the SD of three measurements.

distinguished the mutated sequence from the wild type sequence at the single base resolution (Figure 2e right). In addition, the system was also proved to be able to recognize ssDNA targets by successful detection of a truncated ssDNA of CTNNB1 that contains a S37F mutation. We further proved that the oxygen production is dependent on the presence of the target, the Cas12a enzyme, as well as the specific guide RNA (Figure 2f).

Cas12a-based visual detection of SNV on the MAV-Chip. After validation of the BDNP Conjugation and Cas12a-based cleavage of the reporter, we then tried to employ the modified Cas12a detection system in the MAV-Chip platform. Firstly, to evaluate the uniformity of the MAV-Chip, a uniform concentration of bare PtNPs (2 nM) was loaded into five of the six reaction wells of the chip individually and PBS was loaded into the remaining reaction well as a negative control. The topplate of the chip was shifted vertically to mix the PtNPs in individual reaction wells with 35% H_2O_2 to generate oxygen. Uniform readout distances were observed as expected (Figure S5). Next, we chose a pair of target DNA, i.e., truncated CTNNB1-S37F mutant dsDNA as the target and its corresponding wild type dsDNA as the negative control, to evaluate performance of the modified Cas12a detection system on the MAV-Chip. As shown in Figure 3a, b, CTNNB1-S37F mutant group resulted in long and uniform readout distances while the wild type DNA resulted in readout distances of nearly zero. We found that pre-incubation with BSA in the reaction wells before loading the reaction mixtures could significantly reduce non-specific binding of the BDNPs on the surfaces of the top reaction wells thus significantly reduce background signals (Figure S6). Cleavage time were optimized by comparing signal-to-noise ratios (ratio of the readout distance of mutant DNA to the readout distance of control wild type DNA) of 30 minutes, 60 minutes and 120 minutes of cleavage assays. The biggest signal-to-noise ratio was obtained in 60 minutes assay (data not shown). This assay time was then adopted by following on-chip assays.

To demonstrate multiplicity of the MAV-Chip, we chose four SNVs that are frequently detected in liver cancer (i.e., CTNNB1-S37F, CTNNB1-S45F, P53-R273C and P53-R273H)[28] as targets and their corresponding wild type DNAs as controls to perform the modified Cas12a-based detection assays on the MAV-Chip as well as the conventional Cas12a-based detection assays in microplate using fluorescent reporter, as described in the literature[17]. All the four mutant alleles were successfully detected by both methods, while the wild type alleles showed negative signals in both types of assays (Figure 3c, d). We noticed that different SNVs resulted in slight differences on the bar chart length on the MAV-Chip as well as on the fluorescence intensity in the microplate, which may be owing to different binding kinetics between different targets and their guide RNAs.

To evaluate the sensitivity of the MAV-Chip, mutant DNAs of each target were spiked in their corresponding wild type DNAs (200 nM) with a series of ratios (i.e., 0%, 0.01%, 0.1%, 0.5%, 1%, 10%) and test on the MAV-Chip. As the

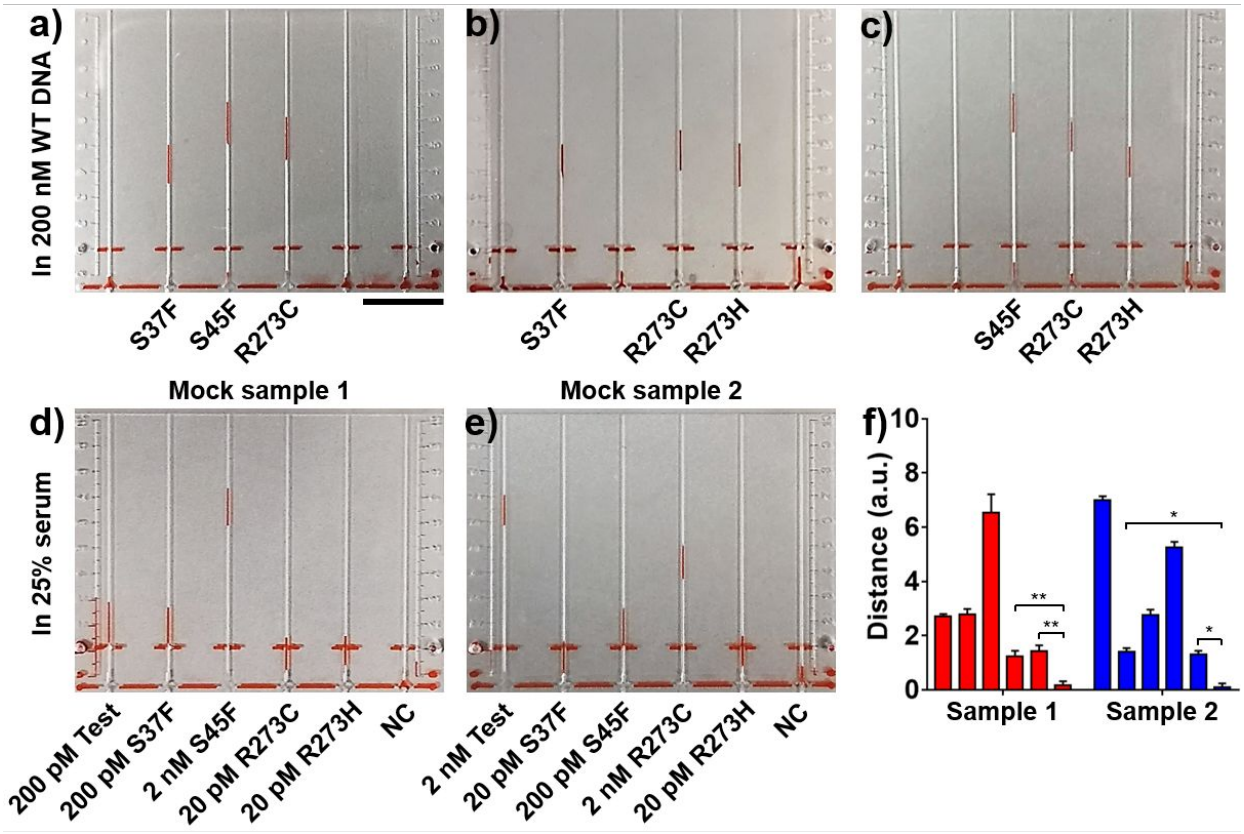


Figure 4. Multiplex detection of cancer-related SNVs in wild-type-DNA spike-in samples and serum spike-in samples. (a-c) Multiplex detection of the cancer-related SNVs in wild-type-DNA spike-in samples. CrRNAs of CTNNB1-S37F, CTNNB1-S45F, P53-R273C and P53-R273H were applied in lane 2-5 (from left to right) of each chip, respectively. Lane 1 and lane 6 served as negative controls as no CrRNA was applied in them. Three of the four dsDNAs each containing a SNV (2 nM), as indicated in (a-c), were mixed and spiked in the mixture of their corresponding wild type DNAs (200 nM final concentrations each) to serve as samples for the multiplex detection. (d-f) Multiplex detection of the cancer-related SNVs in mock cfDNA samples spiked in human serum. CrRNAs of Test, CTNNB1-S37F, CTNNB1-S45F, P53-R273C and P53-R273H were applied in lane 1-5 (from left to right) of each chip, respectively. Lane 6 served as a negative control with no CrRNA applied. Mixtures containing various concentrations of SNV dsDNA, 200 nM of each wild type DNA and 25% human serum were used as mock cfDNA samples for the detection. Scale bar is 1 cm for (a-e). (f), n = three technical replicates, two-tailed Student's t test; *P<0.05, **P<0.01; error bars in (b), (d) and (f) represent the SD of three measurement.

concentration of the target DNA increased, the signal advancement of the MAV-Chip bar charts exhibited correlated increase (Figure 3e, f). The detection limits for all the four liver cancer related mutations were evaluated either by the modified Cas12a-based detection assays on the MAV-Chip (Figure S7) or by the conventional fluorescent reporter-based detection approach (Figure S8). For the MAV-Chip-based approach, three of the four SNVs (i.e. CTNNB1-S37F, CTNNB1-S45F, P53-R273C) were detected at a spike-in ratio as low as 0.01%, and P53-R273H was detected at a spike-in ratio of 0.1%. The detection limits of fluorescent reporter-based approach is ~0.1%, which are consistent with the data from literature[16]. These results suggest that MAV-Chip-based approach is competent for detection of SNVs at low allelic fractions in the clinically relevant range[29].

Multiplex detection of cancer-related SNVs in simulated samples. Detection of cancer mutations in cfDNA samples has shown increasing significance in clinic for both diagnostic and prognostic purposes[30]. To illustrate the application of MAV-Chip platform in detection of cancer mutations, we performed multiplex detection of the four liver cancer-related SNVs in two types of samples on the MAV-Chips (Figure 4). For each sample in the first group, three of the four dsDNAs each containing a SNV (2 nM) were mixed and spiked in the mixture of their corresponding wild type DNAs (200 nM final concentrations each). In a detection assay on a MAV-Chip, guide RNAs targeting the four SNVs and two negative controls without guide RNAs were applied to six different reactions respectively while the same sample was used for all the six reactions. For the three samples in this group, all of the three presented SNVs in each sample were detected while the other absent SNV and the two negative controls were not detected, as expected (Figure 4a-c). In the second group, to further mimic clinical serum samples, two mock serum cfDNA samples were prepared by mixing the four dsDNAs containing liver cancer SNVs and the Test dsDNA as a positive control at different concentrations with all wild type DNAs (200 nM each) and human serum (with a final concentration of 25%). All of the mutations presented in the mock samples were successfully detected and their concentrations quantified from the MAV-Chip readout were near the actual concentrations, which demonstrates the great potential of MAV-Chip in quantification of real cfDNA samples (Figure 4d-f). Results obtained by MAV-Chips were also validated by conventional FQ-labeled reporter-based Cas12a detection assays (Figure S9). The two

series of results are mainly consistent but fluorescence-based assays failed in detecting R273C and R273H at 20 pM.

Conclusion

Current CRISPR/Cas-based nucleic acid detection systems mainly rely on fluorescent reporters or lateral flow strips for readout. The former requires a fluorescent reader for quantification while the later generally provides qualitative results. Both of them provide insufficient quantification capability at the point of care. The integration of platinum nano-reporter and MAV-Chip into CRISPR-Cas12a nucleic acid detection system enables rapid, quantitative and instrument-free detection of SNVs in the high concentration DNA background. Owing to the target DNA-activated indiscriminate single-stranded DNase activity of Cas12a, one type of BDNP can serve as a universal reporter for detection of all targets. Only different guide RNAs need to be specifically designed for detecting different targets. The platinum nano-reporter is also stable, as no significant loss of functionality was observed in at least three months during the experiments if preserved in 1% BSA and stored at 4 ℃. Although we only applied Cas12a as the sensing enzyme, other Cas family enzymes that have been reported for nucleic acid detection (i.e., Cas13a, Cas13b and Cas12b) could also be applied in our platform by adjusting the linker in BDNPs. The platform can be applied in point-of-care quantification of SNVs/SNPs for disease diagnosis and genotyping, as well as point-of-care quantification of other types of nucleic acids, which do not require single-base resolution and could be even less challenging. Furthermore, this platform can analyze complex biospecimen like serum samples without nucleic acid extraction while not compromising sensitivity of the detection, which is an added advantage for point-of-care applications. Although no pre-amplification was performed before MAV-chip detection currently, it may further increase the assay sensitivity if integrated[16]. As a promising tool for next-generation nucleic acid detection, the CRISPR-Cas system has a great potential to be combined with other technologies to enhance its performance and broaden its applications. It could be combined with existing nucleic acid amplification technologies (e.g., RPA, RCA, LAMP, etc.) for better sensitivity, as well as existing nucleic acid detection platforms such as digital PCR, sequencing, electrochemical and colorimetric detection methods for broader applications. It could even be used in detection of proteins by detecting DNA barcodes labelled on antibodies, using the similar formats for immuno-PCR and digital ELISA. Our demonstration of combining CRISPR-Cas12a detection with microfluidics and platinum nano-reporter for point of care detection of SNVs could expand to other types of designs and integrations.

ASSOCIATED CONTENT

Supporting Information

The Supporting Information is available free of charge on the ACS Publications website.

Materials including DNA and guide RNA sequences, detailed experimental procedures, Supplementary Figures (Figure S1-S8) and legends, and related references are included in the Surpporting Information.

AUTHOR INFORMATION

Corresponding Author

* Lidong Qin (lqin@houstonmethodist.org)

Author Contributions

‡ These authors contributed equally to this work.

Notes

The authors declare no competing financial interest.

ACKNOWLEDGMENT

We are grateful for the funding support from NIH-R01 DA035868 and R01 CA180083.

REFERENCES

(1) Veltman, J. A.; Brunner, H. G. *Nat. Rev. Genet.* **2012**, *13*, 565-575.
(2) Dawson, S. J.; Tsui, D. W.; Murtaza, M.; Biggs, H.; Rueda, O. M.; Chin, S. F.; Dunning, M. J.; Gale, D.; Forshew, T.; Mahler-Araujo, B.; Rajan, S.; Humphray, S.; Becq, J.; Halsall, D.; Wallis, M.; Bentley, D.; Caldas, C.; Rosenfeld, N. *N. Engl. J. Med.* **2013**, *368*, 1199-1209.
(3) Syvanen, A. C. *Nat. Rev. Genet.* **2001**, *2*, 930-942.
(4) Genomes Project, C.; Abecasis, G. R.; Auton, A.; Brooks, L. D.; DePristo, M. A.; Durbin, R. M.; Handsaker, R. E.; Kang, H. M.; Marth, G. T.; McVean, G. A. *Nature* **2012**, *491*, 56-65.
(5) Robledo, D.; Palaiokostas, C.; Bargelloni, L.; Martinez, P.; Houston, R. *Rev. Aquac.* **2018**, *10*, 670-682.
(6) He, J.; Zhao, X.; Laroche, A.; Lu, Z. X.; Liu, H.; Li, Z. *Front. Plant Sci.* **2014**, *5*, 484.
(7) Guirgis, B. S.; Abbas, R. O.; Azzazy, H. M. *Int. J. Infect. Dis.* **2010**, *14*, e941-953.
(8) Castle, P. E.; Stoler, M. H.; Wright, T. C., Jr.; Sharma, A.; Wright, T. L.; Behrens, C. M. *Lancet Oncol.* **2011**, *12*, 880-890.
(9) Ross, P.; Hall, L.; Smirnov, I.; Haff, L. *Nat. Biotechnol.* **1998**, *16*, 1347-1351.
(10) Marras, S. A.; Kramer, F. R.; Tyagi, S. *Genet. Anal.* **1999**, *14*, 151-156.
(11) Carter, S. L.; Cibulskis, K.; Helman, E.; McKenna, A.; Shen, H.; Zack, T.; Laird, P. W.; Onofrio, R. C.; Winckler, W.; Weir, B. A.; Beroukhim, R.; Pellman, D.; Levine, D. A.; Lander, E. S.; Meyerson, M.; Getz, G. *Nat. Biotechnol.* **2012**, *30*, 413-421.
(12) Wagle, N.; Berger, M. F.; Davis, M. J.; Blumenstiel, B.; Defelice, M.; Pochanard, P.; Ducar, M.; Van Hummelen, P.; Macconaill, L. E.; Hahn, W. C.; Meyerson, M.; Gabriel, S. B.; Garraway, L. A. *Cancer Discov.* **2012**, *2*, 82-93.
(13) Miotke, L.; Lau, B. T.; Rumma, R. T.; Ji, H. P. *Anal. Chem.* **2014**, *86*, 2618-2624.
(14) Shin, G. W.; Chung, B.; Jung, G. Y.; Jung, G. Y. *Electrophoresis* **2014**, *35*, 1004-1016.
(15) Kong, J.; Zhu, J.; Keyser, U. F. *Chem. Commun. (Camb)* **2017**, *53*, 436-439.
(16) Gootenberg, J. S.; Abudayyeh, O. O.; Lee, J. W.; Essletzbichler, P.; Dy, A. J.; Joung, J.; Verdine, V.; Donghia, N.; Daringer, N. M.; Freije, C. A.; Myhrvold, C.; Bhattacharyya, R. P.; Livny, J.; Regev, A.; Koonin, E. V.; Hung, D. T.; Sabeti, P. C.; Collins, J. J.; Zhang, F. *Science* **2017**, *356*, 438-442.
(17) Chen, J. S.; Ma, E.; Harrington, L. B.; Da Costa, M.; Tian, X.; Palefsky, J. M.; Doudna, J. A. *Science* **2018**, *360*, 436-439.
(18) Gootenberg, J. S.; Abudayyeh, O. O.; Kellner, M. J.; Joung, J.; Collins, J. J.; Zhang, F. *Science* **2018**, *360*, 439-444.
(19) Li, S. Y.; Cheng, Q. X.; Wang, J. M.; Li, X. Y.; Zhang, Z. L.; Gao, S.; Cao, R. B.; Zhao, G. P.; Wang, J. *Cell Discov.* **2018**, *4*, 20.
(20) Myhrvold, C.; Freije, C. A.; Gootenberg, J. S.; Abudayyeh, O. O.; Metsky, H. C.; Durbin, A. F.; Kellner, M. J.; Tan, A. L.; Paul, L. M.; Parham, L. A.; Garcia, K. F.; Barnes, K. G.; Chak, B.; Mondini, A.; Nogueira, M. L.; Isern, S.; Michael, S. F.; Lorenzana, I.; Yozwiak, N. L.; MacInnis, B. L., et al. *Science* **2018**, *360*, 444-448.
(21) Song, Y.; Zhang, Y.; Bernard, P. E.; Reuben, J. M.; Ueno, N. T.; Arlinghaus, R. B.; Zu, Y.; Qin, L. *Nat. Commun.* **2012**, *3*, 1283.
(22) Song, Y.; Wang, Y.; Qin, L. *J. Am. Chem. Soc.* **2013**, *135*, 16785-16788.

(23) Song, Y.; Xia, X.; Wu, X.; Wang, P.; Qin, L. *Angew. Chem. Int. Ed. Engl.* **2014**, *53*, 12451-12455.
(24) Li, Y.; Xuan, J.; Song, Y.; Qi, W.; He, B.; Wang, P.; Qin, L. *ACS Nano* **2016**, *10*, 1640-1647.
(25) Hurst, S. J.; Lytton-Jean, A. K.; Mirkin, C. A. *Anal. Chem.* **2006**, *78*, 8313-8318.
(26) Li, F.; Zhang, H.; Dever, B.; Li, X. F.; Le, X. C. *Bioconjug. Chem.* **2013**, *24*, 1790-1797.
(27) Demers, L. M.; Mirkin, C. A.; Mucic, R. C.; Reynolds, R. A., 3rd; Letsinger, R. L.; Elghanian, R.; Viswanadham, G. *Anal. Chem.* **2000**, *72*, 5535-5541.
(28) Ikeda, S.; Lim, J. S.; Kurzrock, R. *Mol. Cancer Ther.* **2018**, *17*, 1114-1122.
(29) Diaz, L. A., Jr.; Bardelli, A. *J. Clin. Oncol.* **2014**, *32*, 579-586.
(30) Schwarzenbach, H.; Hoon, D. S.; Pantel, K. *Nat. Rev. Cancer* **2011**, *11*, 426-437.

For Table of Contents Only

